

Investigation on Thermomechanical Bending of Functionally Graded Sandwich Plates Using a Novel Combined 2D Integral Plate Model

H. Belarbi¹, B. Boucham¹, F. Bourada^{2*}, A. Kaci^{2,3}, M. Bourada², and A. Tounsi^{2,4,5,6}

¹Laboratory of Mechanics of Structures and Solids, Faculty of Technology,
Department of Mechanical Engineering, University of Sidi Bel Abbes, Sidi Bel Abbes, 22000 Algeria

²Material and Hydrology Laboratory, Faculty of Technology, Civil Engineering Department,
University of Sidi Bel Abbes, Sidi Bel Abbes, 22000 Algeria

³Department of Civil and Hydraulic Engineering, Faculty of Technology,
Dr. Tahar Moulay University of Saida, Saida, 20000 Algeria

⁴Department of Civil and Environmental Engineering, King Fahd University of Petroleum and Minerals,
Dhahran, 31261 Saudi Arabia

⁵Department of Civil and Environmental Engineering, Lebanese American University, P.O. Box 36, Byblos, Lebanon

⁶Interdisciplinary Research Center for Construction and Building Materials, King Fahd University
of Petroleum and Minerals, Dhahran, 31261 Saudi Arabi

* e-mail: bouradafouad@yahoo.fr

Received November 21, 2023; revised December 31, 2023; accepted January 10, 2024

Abstract—This study presents the flexural analysis of Ti-6Al-4V/ZrO₂ functionally graded (FG) sandwich plates under combined thermal and mechanical loading via exponential-cubic-sinusoidal integral shear deformation theory. The current formulation used in the modeling provides a parabolic distribution of transverse shear stresses without requiring additional factors in the formulation. Various sandwich plate models with different layer thicknesses and material types are considered. The FG layers vary continuously and smoothly according to exponential and power-law functions. The governing differential equations of the system are derived and solved analytically using the virtual work principle and Navier's approach. Benchmark comparisons are performed to validate and show the accuracy of the proposed model. Various parametric examples are presented to illustrate the effect of the geometry, dimensions, FG sandwich type and material gradient on the static flexural response of the studied structure.

Keywords: FG sandwich plate, gradient, four-variable integral plate model, thermomechanical bending, deflection and stresses, virtual work principle, Navier's approach

DOI: 10.1134/S1029959924040118

1. INTRODUCTION

Sandwich structures occupy an important place in the manufacture of composite parts. They are present in practically all fields of application. These structures are fabricated by gluing or welding two thin skins on a lighter-weight core with weaker mechanical characteristics, which maintains spacing between the skins and transfers mechanical loads by shear from one skin to the other. Such a structure has very high strength/mass and stiffness/mass ratios in bending. There are various models of sandwich structures. The most recognized and widely used one is a sandwich structure with three homogeneous layers (core and face sheets). A growing trend is the introduction

of advanced composite materials in the manufacture of sandwich plates. The incorporation of FG and sandwich structures in the construction sectors has increased considerably to overcome the problem of conventional structures and materials related to their low resistance to high temperatures [1–3]. We find in the literature sandwich plates with faces made of functionally graded material (FGM) and an isotropic core [4–6] or with homogeneous face sheets and an FG core [6–9].

Numerous studies of sandwich panels with FGM face sheets have been made with regard to their use in the design of engineered structures. Analysis of the thermal buckling response of sandwich plates with

two FGM faces and a homogeneous central core was presented in [5] using the theory of sinusoidal shear strain. Natarajan and Ganapathi [10] analyzed the static bending and vibrational response of two types of FGM sandwich plates composed of homogeneous face sheets with an FGM core and FGM face sheets with a homogeneous hard core. The analysis was performed using a model of higher-order shear deformation theory (HSDT) and a QUAD-8 shear flexible element. A higher-order theory of shear deformation by thickness stretching was applied by Neves et al. [11] to analyze various behaviors of two FG sandwich models. An analytical model for the response analysis of FG sandwich structures with an isotropic middle layer was proposed by Thai et al. [12] with taking into account the boundary conditions. The dynamic and static behaviors of 2D FG and isotropic sandwich structures were studied by Nguyen et al. [13] for fully FG plates and two sandwich models, one with an FG core and the other with FGM skins. Akavci [14] presented a new theory of quasi-3D shear and normal deformation of plates with a hyperbolic warping function for various responses (stability, static, dynamic) using FG sandwich plates with an FG core or FG face sheets.

Thermomechanical behavior is due to the combination of mechanical and thermal loads simultaneously. This type of loading is common in structures used in the aircraft, ship building, marine industries, automotive and civil engineering, and it is necessary to examine their responses under such loading conditions. There are few works that study the bending behavior of graded sandwich structures under various types of load (mechanical/thermal). Zenkour and Alghamdi [15] investigated the flexural behavior of 2D graded sandwich structures with a ceramic core and FG skins subjected to thermomechanical loads. Wang and Shen [16] studied the nonlinear behavior (buckling, vibration, bending) of an FG sandwich subjected to thermal environment and resting on an elastic foundation.

Some authors are also interested in crack and fracture problems in the structures. For example, Hiranaiyah et al. [17] investigated the thermomechanical dynamic response and stability of imperfect FG sandwich plates with geometric discontinuity and physical neutral surface. Kanu et al. [18] discussed the effect of fracture on the mechanical behavior of FG structures and materials. Based on the finite element method, Abbas and Razavi [19] examined the thermoelastic response of a fiber-reinforced anisotropic material by considering a crack problem. Petrova and

Schmauder [20] modeled and studied the thermomechanical fracture of an FG structure taking into account multiple crack interaction. Abouelregal et al. [21] proposed a generalized heat equation for a temperature-dependent nonsimple thermoelastic cylinder with including the Caputo–Fabrizio fractional derivative. Based on an extension of the Fourier approach, the Atangana–Baleanu operator, and a novel nonlocal single core, Atta [22] investigated a thermoelastic medium with a spherical cavity within the framework of partial elastic thermal diffusion theory. Based on the Hermite–Ritz method and classical beam theory, Jena et al. [23] studied the effect of the presence of an elastic substrate on the vibrational characteristics of an imperfect FG beam, taking into account the small scale effect via bi-Helmholtz nonlocal elasticity. Many studies are devoted to the investigation of the thermal and thermomechanical response [24, 25].

The development of different theories to predict the behavior of FG structures has increased because of their wide use in the field of engineering structures. There are several plate theories developed to analyze FG materials. The classical model (classical plate theory (CPT)) is an extension of the Kirchhoff–Love hypothesis for slender and thin isotropic structures [26–28]. However, it cannot be applied for short and thick FG structures as it takes no account of the shear effect. The second model proposed by Reissner–Mindlin is called the first-order shear deformation theory (FSDT). The accuracy of its solutions depends heavily on the prediction of the best estimates for the shear correction factors to correct uniform shear stresses across the entire thickness of the structure [29–32]. The CPT and FSDT theories were shown to be inadequate for computing accurate solutions of FG plates. Another option is the refined higher-order shear deformation theory (HSDT) [33–40]. This model does not need any correction factors and can more accurately predict the behavior of moderate and thick FG plates. However, a larger number of unknown variables in the displacement field in HSDT leads to higher computational costs.

Here we develop a combined four-variable integral model with the aim to reduce the number of unknown variables and computational cost, to obtain accurate results, and to process several types of FG sandwich plates. The thermomechanical bending response of 2D FG sandwich structures is investigated analytically using the model.

The proposed combined exponential-cubic-sinusoidal integral shear deformation theory contains

only four variable functions, and therefore its governing equations are reduced compared to other similar solutions. The model takes into account the transverse shear deformation effect in a parabolic manner along the thickness direction and satisfies the stress-free boundary conditions on nonplate surfaces without any requirement for shear correction factors. The equations of stability are derived from the virtual work principle. Navier’s technique is applied to obtain the closed form. The numerical values of displacements and stresses obtained with the current theory are verified and compared with various existing solutions. Finally, the effects of certain parameters, such as the load type (transversal and thermal), volume fraction, thermal load, layer-to-thickness ratio and other dimensions, on the sandwich structure response are studied.

2. MATHEMATICAL MODELING

2.1. FG Sandwich Geometry

In this work, various uniform sandwich plates are considered. The geometry and dimensions are presented in Fig. 1. The plate is made of Ti-6Al-4V/ZrO₂ (metal/ceramic) and contains three layers, which are either homogeneous or functionally graded, as presented in Sect. 5.

2.1.1. FG Face Sheets

The properties (E , ν and α) of the face sheet layers are calculated as [41, 42]:

$$\begin{aligned} E^{(1,3)} &= E_m + (E_c - E_m)V^{(1,3)}, \\ \alpha^{(1,3)} &= \alpha_m + (\alpha_c - \alpha_m)V^{(1,3)} \end{aligned} \quad (1)$$

with

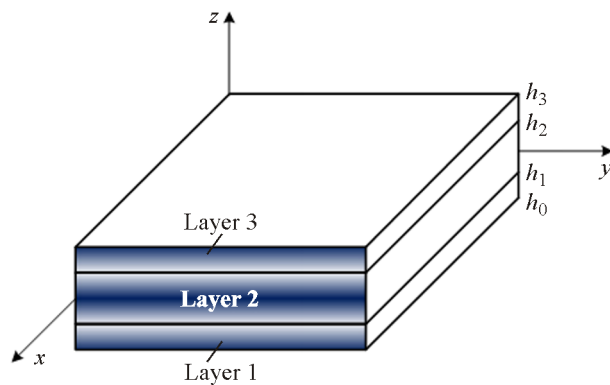


Fig. 1. Geometry of a three-layered FG sandwich plate.

$$V^{(1)} = \left(\frac{z - h_0}{h_1 - h_0} \right)^{p_{fs}}, \quad z \in [h_0, h_1], \quad (2)$$

$$V^{(3)} = \left(\frac{z - h_3}{h_2 - h_3} \right)^{p_{fs}}, \quad z \in [h_2, h_3].$$

The subscripts c and m correspond to the used ceramic or metal material. The exponent p_{fs} is the gradient index, and $V^{(1,3)}$ is the volume fraction of the 1st and 3rd layers.

2.1.2. FG Core

In contrast to the face sheet properties, the properties of the FG core vary as exponential function:

$$E^{(2)} = E_m \exp \left(\ln \left(\frac{E_c}{E_m} \right) V^{(2)} \right), \quad (3)$$

$$V^{(2)} = \left(\frac{2|z|}{h_2 - h_1} \right)^{p_{core}}, \quad z \in [h_1, h_2],$$

where p_{core} is the core gradient index.

The thickness ratios of the three layers of FG sandwich plates are summarized in Table 1.

2.2. Kinematics

It is assumed that the straight section is perpendicular to the neutral axis, but loses its perpendicularity and flatness after deformation according to the conventional HSDT theories. The displacement field of HSDT contains five unknown variables and is given as follows [43]:

$$\begin{aligned} u(x, y, z) &= u_0(x, y) - z \frac{\partial w_0(x, y)}{\partial x} + f(z)\varphi_x(x, y), \\ v(x, y, z) &= v_0(x, y) - z \frac{\partial w_0(x, y)}{\partial y} \\ &\quad + f(z)\varphi_y(x, y), \\ w(x, y, z) &= w_0(x, y), \end{aligned} \quad (4)$$

where u_0 , v_0 , w_0 , φ_x , φ_y are the five unknown displacement functions of the mid-plane of the plate.

Unlike the analytical theory used for thin structures which neglects the transverse shear effect as the

Table 1. Estimates of parameters h_0 , h_1 , h_2 and h_3 for different FG sandwich plates

Layer thickness ratio	h_0	h_1	h_2	h_3
1-1-1	$-h/2$	$-h/6$	$h/6$	$h/2$
1-2-1	$-h/2$	$-h/4$	$h/4$	$h/2$
2-1-2	$-h/2$	$-h/10$	$h/10$	$h/2$

classical theory and unlike the FSDT that assumes constant shear stresses across the thickness and the HSDT theories containing a larger number of variables, the developed model based on the section that loses its perpendicularity and flatness after deformation gives a parabolic variation of transverse shear stresses through the thickness, ensures their equality to zero on the upper and lower surfaces without requiring any correction factors, and contains only four unknown variables. By changing

$$\varphi_x = \zeta_1 \int \theta(x, y) dx \text{ and } \varphi_y = \zeta_2 \int \theta(x, y) dy,$$

the integral displacement fields can be simplified as follows:

$$\begin{aligned} u(x, y, z) &= u_0(x, y) - z \frac{\partial w_0}{\partial x} + \zeta_1 f(z) \int \theta(x, y) dx, \\ v(x, y, z) &= v_0(x, y) - z \frac{\partial w_0}{\partial y} + \zeta_2 f(z) \int \theta(x, y) dy, \\ w(x, y, z) &= w_0(x, y). \end{aligned} \tag{5}$$

The constants ζ_1 and ζ_2 depend on the geometry.

In the current study, the shape functions $f(z)$ take a combined form (exponential-cubic-trigonometric) and satisfy the stress-free boundary conditions, with

$$\begin{aligned} f(z) &= z \left(e^{-2z^2/h^2} + \left(1 - \frac{4}{3} \left(\frac{z}{h} \right)^2 \right) - \frac{h}{\pi z} \sin \left(\frac{\pi z}{h} \right) \right), \\ g(z) &= 1 + e^{-2z^2/h^2} - \frac{4z^2 e^{-2z^2/h^2}}{h^2} - 4 \left(\frac{z}{h} \right)^2 - \cos \left(\frac{\pi z}{h} \right). \end{aligned} \tag{6}$$

By deriving the displacement field, we obtain the strain field as

$$\begin{aligned} \begin{Bmatrix} \varepsilon_x \\ \varepsilon_y \\ \gamma_{xy} \end{Bmatrix} &= \begin{Bmatrix} \varepsilon_x^0 \\ \varepsilon_y^0 \\ \gamma_{xy}^0 \end{Bmatrix} + z \begin{Bmatrix} k_x^b \\ k_y^b \\ k_{xy}^b \end{Bmatrix} + f(z) \begin{Bmatrix} k_x^s \\ k_y^s \\ k_{xy}^s \end{Bmatrix}, \\ \begin{Bmatrix} \gamma_{yz} \\ \gamma_{xz} \end{Bmatrix} &= g(z) \begin{Bmatrix} \gamma_{yz}^0 \\ \gamma_{xz}^0 \end{Bmatrix}, \end{aligned} \tag{7}$$

where

$$\begin{Bmatrix} \varepsilon_x^0 \\ \varepsilon_y^0 \\ \gamma_{xy}^0 \end{Bmatrix} = \begin{Bmatrix} \frac{\partial u_0}{\partial x} \\ \frac{\partial v_0}{\partial y} \\ \frac{\partial u_0}{\partial y} + \frac{\partial v_0}{\partial x} \end{Bmatrix}, \quad \begin{Bmatrix} k_x^b \\ k_y^b \\ k_{xy}^b \end{Bmatrix} = \begin{Bmatrix} -\frac{\partial^2 w_0}{\partial x^2} \\ -\frac{\partial^2 w_0}{\partial y^2} \\ -2 \frac{\partial^2 w_0}{\partial x \partial y} \end{Bmatrix},$$

$$\begin{Bmatrix} k_x^s \\ k_y^s \\ k_{xy}^s \end{Bmatrix} = \begin{Bmatrix} \zeta_1 \theta \\ \zeta_2 \theta \\ \zeta_1 \frac{\partial}{\partial y} \int \theta dx + \zeta_2 \frac{\partial}{\partial x} \int \theta dy \end{Bmatrix}, \tag{8}$$

$$\begin{Bmatrix} \gamma_{yz}^0 \\ \gamma_{xz}^0 \end{Bmatrix} = \begin{Bmatrix} \zeta_2 \int \theta dy \\ \zeta_1 \int \theta dx \end{Bmatrix},$$

and $g(z)$ is given as follows:

$$g(z) = \frac{df(z)}{dz}. \tag{9}$$

The integrals appearing in the above expressions must be solved by a Navier-type solution and can be expressed as

$$\begin{aligned} \frac{\partial}{\partial y} \int \theta dx &= \chi \frac{\partial^2 \theta}{\partial x \partial y}, \quad \frac{\partial}{\partial x} \int \theta dy = \psi \frac{\partial^2 \theta}{\partial x \partial y}, \\ \int \theta dx &= \chi \frac{\partial \theta}{\partial x}, \quad \int \theta dy = \psi \frac{\partial \theta}{\partial y}, \end{aligned} \tag{10}$$

with

$$\chi = -\frac{1}{\alpha^2}, \quad \psi = -\frac{1}{\beta^2}, \quad \zeta_1 = \alpha^2, \quad \zeta_2 = \beta^2. \tag{11}$$

2.3. Constitutive Equations

The stress-strain relationships can be expressed as

$$\begin{Bmatrix} \sigma_x \\ \sigma_y \\ \tau_{xy} \\ \tau_{xz} \\ \tau_{yz} \end{Bmatrix}^{(n)} = \begin{bmatrix} C_{11} & C_{12} & 0 & 0 & 0 \\ C_{12} & C_{22} & 0 & 0 & 0 \\ 0 & 0 & C_{66} & 0 & 0 \\ 0 & 0 & 0 & C_{55} & 0 \\ 0 & 0 & 0 & 0 & C_{44} \end{bmatrix}^{(n)} \begin{Bmatrix} \varepsilon_x - \alpha(z)T(z) \\ \varepsilon_y - \alpha(z)T(z) \\ \gamma_{xy} \\ \gamma_{xz} \\ \gamma_{yz} \end{Bmatrix}^{(n)}, \tag{12}$$

where $\varepsilon_x, \varepsilon_y, \gamma_{xy}, \gamma_{xz}, \gamma_{yz}$ and $\sigma_x, \sigma_y, \tau_{xy}, \tau_{xz}, \tau_{yz}$ are the strain and stress components, respectively.

The elastic constants of the n th layer are

$$\begin{aligned} C_{11}^{(n)} &= C_{22}^{(n)} = \frac{E^{(n)}(z)}{1-\nu^{(n)2}}, \quad C_{12}^{(n)} = \frac{\nu E^{(n)}(z)}{1-\nu^{(n)2}}, \\ C_{44}^{(n)} &= C_{55}^{(n)} = C_{66}^{(n)} = \frac{E^{(n)}(z)}{2(1+\nu^{(n)})}. \end{aligned} \tag{13}$$

3. GOVERNING EQUATIONS

The virtual work principle [44–46] is applied for a static thermomechanical problem of an FG sandwich plate:

$$\delta U + \delta V = 0. \tag{14}$$

After replacing the virtual strain energy δU and the virtual work δV done by applied forces in the above equation, the principle of virtual work takes the following form:

$$\int_A [N_x \delta \varepsilon_x^0 + N_y \delta \varepsilon_y^0 + N_{xy} \delta \gamma_{xy}^0 + M_x^b \delta k_x^b + M_y^b \delta k_y^b + M_{xy}^b \delta k_{xy}^b + M_x^s \delta k_x^s + M_y^s \delta k_y^s + M_{xy}^s \delta k_{xy}^s + S_{yz}^s \delta \gamma_{yz}^0 + S_{xz}^s \delta \gamma_{xz}^0] d\Omega - \int_{\Omega} q w d\Omega = 0, \tag{15}$$

where the stress resultants N , M and S are defined as

$$\begin{pmatrix} N_x & N_y & N_{xy} \\ M_x^b & M_y^b & M_{xy}^b \\ M_x^s & M_y^s & M_{xy}^s \end{pmatrix} = \sum_{n=1}^3 \int_{h_{n-1}}^{h_n} (\sigma_x, \sigma_y, \tau_{xy})^{(n)} \begin{pmatrix} 1 \\ z \\ f(z) \end{pmatrix} dz, \tag{16}$$

$$(S_{xz}^s, S_{yz}^s) = \sum_{n=1}^3 \int_{h_{n-1}}^{h_n} (\tau_{xz}, \tau_{yz})^{(n)} g(z) dz,$$

where the top and bottom z coordinates of the n th layer are h_n and h_{n-1} , and Ω is the top surface.

The static governing equations of the system can be obtained based on the virtual work cited in the above equation as

$$\begin{aligned} \delta u_0: \frac{\partial N_x}{\partial x} + \frac{\partial N_{xy}}{\partial y} &= 0, \\ \delta v_0: \frac{\partial N_{xy}}{\partial x} + \frac{\partial N_y}{\partial y} &= 0, \\ \delta w_0: \frac{\partial^2 M_x^b}{\partial x^2} + 2 \frac{\partial^2 M_{xy}^b}{\partial x \partial y} + \frac{\partial^2 M_y^b}{\partial y^2} + q &= 0, \tag{17} \\ \delta \theta: -\zeta_1 M_x^s - \zeta_2 M_y^s - (\chi \zeta_1 + \psi \zeta_2) \frac{\partial^2 M_{xy}^s}{\partial x \partial y} \\ + \chi \zeta_1 \frac{\partial S_{xz}^s}{\partial x^2} + \psi \zeta_2 \frac{\partial S_{yz}^s}{\partial y^2} &= 0. \end{aligned}$$

The resultants N , M and S can be computed by substituting Eqs. (8), (9) and (13) into Eqs. (17) as follows:

$$\begin{Bmatrix} N \\ M^b \\ M^s \end{Bmatrix} = \begin{bmatrix} A & B & C \\ B & D & F \\ C & F & H \end{bmatrix} \begin{Bmatrix} \varepsilon^{(0)} \\ k^b \\ k^s \end{Bmatrix} - \begin{Bmatrix} N^T \\ M^{bT} \\ M^{sT} \end{Bmatrix}, \tag{18}$$

$$\begin{Bmatrix} S_{yz} \\ S_{xz} \end{Bmatrix} = \begin{bmatrix} A_{44}^s & 0 \\ 0 & A_{55}^s \end{bmatrix} \begin{Bmatrix} \gamma_{yz}^{(0)} \\ \gamma_{xz}^{(0)} \end{Bmatrix},$$

where

$$\begin{aligned} N &= \{N_x, N_y, N_{xy}\}^t, \quad M^b = \{M_x^b, M_y^b, M_{xy}^b\}^t, \\ M^s &= \{M_x^s, M_y^s, M_{xy}^s\}^t, \quad N^T = \{N_x^T, N_y^T, 0\}^t, \\ M^{bT} &= \{M_x^{bT}, M_y^{bT}, 0\}^t, \quad M^{sT} = \{M_x^{sT}, M_y^{sT}, 0\}^t, \tag{19} \\ \varepsilon^{(0)} &= \{\varepsilon_x^{(0)}, \varepsilon_y^{(0)}, \gamma_{xy}^{(0)}\}^T, \end{aligned}$$

$$k^b = \{k_x^b, k_y^b, k_{xy}^b\}^T, \quad k^s = \{k_x^s, k_y^s, k_{xy}^s\}^T$$

with

$$\begin{aligned} &\begin{Bmatrix} A_{11} & B_{11} & D_{11} & C_{11} & F_{11} & H_{11} \\ A_{12} & B_{12} & D_{12} & C_{12} & F_{12} & H_{12} \\ A_{66} & B_{66} & D_{66} & C_{66} & F_{66} & H_{66} \end{Bmatrix} \\ &= \sum_{n=1}^3 \int_{h_{n-1}}^{h_n} C_{11}^{(n)} (1, z, z^2, f(z), z f(z), f^2(z)) \\ &\quad \times \begin{Bmatrix} 1 \\ v \\ \frac{1-v}{2} \end{Bmatrix} dz, \tag{20} \end{aligned}$$

and

$$\begin{aligned} &(A_{22}, B_{22}, D_{22}, B_{22}^s, D_{22}^s, H_{22}^s) \\ &= (A_{11}, B_{11}, D_{11}, B_{11}^s, D_{11}^s, H_{11}^s), \tag{21} \\ &A_{44}^s = A_{55}^s = \sum_{n=1}^3 \int_{h_{n-1}}^{h_n} \frac{E^{(n)}(z)}{2(1+\nu)} [g(z)]^2 dz. \end{aligned}$$

The stress and moment resultants due to thermal loading ($N_x^T, N_y^T, M_x^{bT}, M_y^{bT}, M_x^{sT}$ and M_y^{sT}) are defined by

$$\begin{aligned} &\begin{Bmatrix} N_x^T \\ N_y^T \end{Bmatrix} = \sum_{n=1}^3 \int_{h_{n-1}}^{h_n} \begin{Bmatrix} (C_{11} + C_{12}) \alpha T \\ (C_{12} + C_{22}) \alpha T \end{Bmatrix}^{(n)} dz, \\ &\begin{Bmatrix} M_x^{bT} \\ M_y^{bT} \end{Bmatrix} = \sum_{n=1}^3 \int_{h_{n-1}}^{h_n} \begin{Bmatrix} (C_{11} + C_{12}) \alpha T \\ (C_{12} + C_{22}) \alpha T \end{Bmatrix}^{(n)} z dz, \tag{22} \\ &\begin{Bmatrix} M_x^{sT} \\ M_y^{sT} \end{Bmatrix} = \sum_{n=1}^3 \int_{h_{n-1}}^{h_n} \begin{Bmatrix} (C_{11} + C_{12}) \alpha T \\ (C_{12} + C_{22}) \alpha T \end{Bmatrix}^{(n)} f(z) dz. \end{aligned}$$

The through-thickness variation of temperature $T(x, y, z)$ [30–33] can be expressed in a generalized form as

$$T(x, y, z) = T_1(x, y) + \frac{z}{h}T_2(x, y) + \frac{f(z)}{h}T_3(x, y), \quad (23)$$

where T_1 , z/hT_2 , and $f(z)/hT_3$ are the uniform, linear and nonlinear variation of temperature load through the thickness, with

$$\begin{Bmatrix} T_1 \\ T_2 \\ T_3 \end{Bmatrix} = \begin{Bmatrix} t_1 \\ t_2 \\ t_3 \end{Bmatrix} \sin\left(\frac{m\pi x}{a}\right) \sin\left(\frac{n\pi y}{b}\right). \quad (24)$$

4. CLOSED-FORM SOLUTIONS

The analytical solution used here to solve Eq. (17) is the Navier solution given by [47–51]:

$$\begin{Bmatrix} u_0 \\ v_0 \\ w_0 \\ \theta \end{Bmatrix} = \sum_{m=1}^{\infty} \sum_{n=1}^{\infty} \begin{Bmatrix} U_{mn} \cos(\alpha x) \sin(\beta y) \\ V_{mn} \sin(\alpha x) \cos(\beta y) \\ X_{mn} \sin(\alpha x) \sin(\beta y) \\ Y_{mn} \sin(\alpha x) \sin(\beta y) \end{Bmatrix}, \quad (25)$$

with $\alpha = m\pi/a$ and $\beta = n\pi/b$.

The chosen solution ensures the boundary condition

$$N_x = M_x^b = M_x^s = v_0 = w_0 = \frac{\partial \theta}{\partial y} = 0$$

at $x=0, a$,

$$N_y = M_y^b = M_y^s = u_0 = w_0 = \frac{\partial \theta}{\partial x} = 0$$

at $x=0, b$.

The bi-sinusoidal load can be given as

$$q(x, y) = q_0 \sin\left(\frac{m\pi x}{a}\right) \sin\left(\frac{n\pi y}{b}\right). \quad (27)$$

The final solution of the system can be obtained by substituting Eqs. (19), (20) and (22) into Eqs. (18) and the subsequent results into Eqs. (17):

$$[\mathfrak{R}]\{\Delta\} = \{P\}, \quad (28)$$

where $[\mathfrak{R}]$, $\{\Delta\}$ and $\{P\}$ are the stiffness matrix, displacement and force vectors given by

$$\begin{aligned} \mathfrak{R}_{11} &= A_{11}\alpha^2 + A_{66}\beta^2, \\ \mathfrak{R}_{12} &= \alpha\beta(A_{12} + A_{66}), \\ \mathfrak{R}_{13} &= (B_{12} + 2B_{66})\alpha\beta^2 + B_{11}\beta^3, \\ \mathfrak{R}_{14} &= -(C_{11}\zeta_1 + C_{12}\zeta_2)\alpha - C_{66}(\chi\zeta_1 + \psi\zeta_2)\alpha\beta^2, \\ \mathfrak{R}_{22} &= A_{22}\beta^2 + A_{66}\alpha^2, \\ \mathfrak{R}_{23} &= -B_{22}\beta^3 - (2B_{66} + B_{12})\alpha^2\beta, \end{aligned} \quad (29)$$

$$\mathfrak{R}_{24} = -(C_{12}\zeta_1 + C_{22}\zeta_2)\beta + C_{66}(\chi\zeta_1 + \psi\zeta_2)\alpha^2\beta,$$

$$\mathfrak{R}_{33} = D_{11}\alpha^4 + D_{22}\beta^4 + 2(2D_{66} + D_{12})\alpha^2\beta^2,$$

$$\mathfrak{R}_{34} = 2F_{66}(\chi\zeta_1 + \psi\zeta_2)\alpha^2\beta^2$$

$$+ \zeta_2(F_{12}\alpha^2 + F_{22}\alpha^2) + \zeta_1(F_{11}\alpha^2 + F_{12}\beta^2),$$

$$\mathfrak{R}_{44} = H_{11}\zeta_1^2 + H_{22}\zeta_2^2 + 2H_{12}\zeta_1\zeta_2$$

$$+ H_{66}(\chi\zeta_1 + \psi\zeta_2)^2\alpha^2\beta^2 + A_{55}^s\zeta_1^2\chi^2\alpha^2 + A_{44}^s\zeta_2^2\psi^2\beta^2$$

and

$$\{P_1\} = \alpha(A^T t_1 + B^T t_2 + {}^a B_T t_3),$$

$$\{P_2\} = \beta(A^T t_1 + B^T t_2 + {}^a B_T t_3), \quad (30)$$

$$\{P_3\} = -q_0 - h(\alpha^2 + \beta^2)(B^T t_1 + D^T t_2 + {}^a D_T t_3),$$

$$\{P_4\} = -2h(C^T t_1 + F^T t_2 + {}^a F_T t_3),$$

in which

$$\{A^T, B^T, D^T\} = \sum_{n=1}^3 \int_{h_{n-1}}^{h_n} \frac{E^{(n)}(z)}{1-\nu^{(n)2}}$$

$$\times (1+\nu^{(n)})\alpha^{(n)}\{1, \bar{z}, \bar{z}^2\} dz,$$

$$\{{}^a B_T, {}^a D_T\} = \sum_{n=1}^3 \int_{h_{n-1}}^{h_n} \frac{E^{(n)}(z)}{1-\nu^{(n)2}}$$

$$\times (1+\nu^{(n)})\bar{f}(z)\alpha^{(n)}\{1, \bar{z}\} dz,$$

$$\{C^T, F^T, {}^a F_T\} = \sum_{n=1}^3 \int_{h_{n-1}}^{h_n} \frac{E^{(n)}(z)}{1-\nu^{(n)2}}$$

$$\times (1+\nu^{(n)})\alpha^{(n)}\bar{f}(z)\alpha^{(n)}\{1, \bar{z}, \bar{f}(z)\} dz,$$

where

$$\bar{z} = \frac{z}{h}, \quad \bar{f}(z) = \frac{f(z)}{h}. \quad (32)$$

5. NUMERICAL RESULTS

In this section, the materials used in the FG sandwich plate are ZrO₂ ceramics: Young's modulus $E_c = 117.0$ GPa, thermal expansion coefficient $\alpha_c = 7.11 \times 10^{-6}/\text{K}$ and Poisson's ratio $\nu = 0.3$, and Ti-6Al-4V metal: Young's modulus $E_m = 66.2$ GPa, thermal expansion coefficient $\alpha_m = 10.3 \times 10^{-6}/\text{K}$ and Poisson's ratio $\nu = 0.3$. In order to verify the proposed model, various results are presented, discussed and compared with those found in the published literature. The dimensionless form of the deflection and stresses is given by

$$\bar{w} = \frac{10^3}{q_0 a^4 / (E_0 h^3) + 10^3 \alpha_0 t_2 a^2 / h} w \left(\frac{a}{2}, \frac{b}{2} \right),$$

$$\bar{\sigma}_x = \frac{10}{q_0 a^2 / h^2 + 10 E_0 \alpha_0 t_2 a^2 / h^2} \sigma_x \left(\frac{a}{2}, \frac{b}{2}, z \right),$$

Table 2. Validation of the dimensionless central transverse displacement and axial stresses of an FG sandwich plate with an isotropic core under thermomechanical loading

p_{fs}	Model	$\bar{\sigma}_x$		\bar{w}	
		1-1-1	2-1-2	1-1-1	2-1-2
1	Present	-2.661842	-2.539439	1.010811	1.035752
	SSDPT*	-2.659816	-2.537365	1.011263	1.036213
	FSDPT*	-3.756017	-3.618476	1.132449	1.160568
2	Present	-2.383481	-2.245982	1.067617	1.095612
	SSDPT*	-2.381343	-2.2438	1.068091	1.096094
	FSDPT*	-3.446485	-3.289757	1.195703	1.227765
3	Present	-2.264682	-2.129695	1.091832	1.119306
	SSDPT*	-2.262512	-2.127487	1.092312	1.119793
	FSDPT*	-3.311823	-3.156414	1.223232	1.255041
4	Present	-2.202201	-2.07257	1.104559	1.130939
	SSDPT*	-2.20002	-2.070352	1.105041	1.131428
	FSDPT*	-3.239941	-3.089733	1.237931	1.268689
5	Present	-2.16478	-2.040332	1.112177	1.137502
	SSDPT*	-2.162596	-2.038109	1.11266	1.137993
	FSDPT*	-3.196423	-3.051612	1.246833	1.276497

* Taken from [15].

$$\bar{\tau}_{xy} = \frac{1}{q_0 a/h + E_0 \alpha_0 t_2 a/(10h)} \tau_{xy}(0, 0, z), \quad (33)$$

$$\bar{\tau}_{xz} = \frac{1}{q_0 a/h + E_0 \alpha_0 t_2 a/(10h)} \tau_{xz}\left(0, \frac{b}{2}, z\right),$$

where $q_0 = 100$ Pa, $a/h = 10$, $t_1 = 0$, and $t_2 = t_3 = 100$ K, $E_0 = 1$ GPa, $\alpha_0 = 10^{-6}/K$.

For the validation of the current model based on undetermined integral HSDT theory, the obtained results for the axial stress and central deflection are checked and compared with the existing model [15] based on sinusoidal and first-order shear deformation theory. The validation results in Table 2 are obtained for layer thickness ratios of 1-1-1 and 2-1-2 and the face sheet gradient indices 1, 2, 3, 4 and 5. It is clearly seen that the model results are in excellent agreement with the results obtained in [15] with the model of sinusoidal shear deformation plate theory. The difference between the FSDT theory (Reissner–Mindlin model) and the current model is due to the uniform shear stress distribution across the thickness assumed by the FSDT model. We can also conclude that the 1-1-1 sandwich plate gives smaller values of the central deflection because the core layer is most rigid and occupies a third of the total thickness of the structure.

Table 3 presents the results for the dimensionless central deflection and stresses along the x axis as functions of the layer thickness and the face sheet

Table 3. Nondimensional central transverse displacement and axial stresses of a sandwich structure with three FG layers under thermomechanical loading

p_{fs}	Layer thickness ratio	\bar{w}	$\bar{\sigma}_x$
1	1-1-1	1.015543	-2.639647
	1-2-1	0.984386	-2.792744
	2-1-2	1.036949	-2.534229
2	1-1-1	1.073225	-2.357006
	1-2-1	1.034491	-2.547521
	2-1-2	1.097021	-2.239752
3	1-1-1	1.097852	-2.236173
	1-2-1	1.057294	-2.435772
	2-1-2	1.120807	-2.123015
4	1-1-1	1.110805	-2.172569
	1-2-1	1.070000	-2.373454
	2-1-2	1.132487	-2.065657
5	1-1-1	1.118562	-2.134458
	1-2-1	1.077988	-2.334258
	2-1-2	1.139079	-2.033284

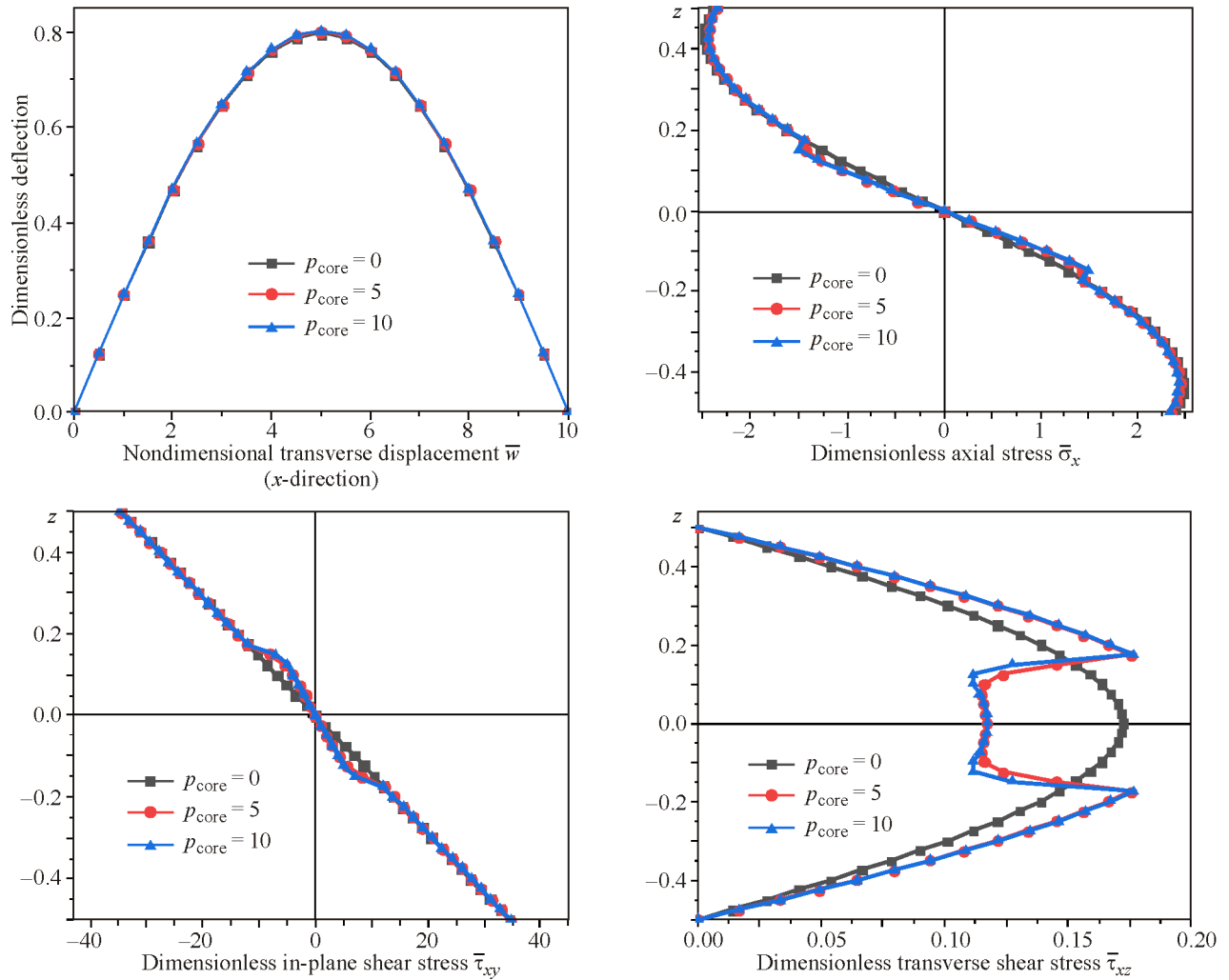


Fig. 2. Effect of the core gradient index p_{core} on the flexural characteristics of a sandwich structure with identical layer thicknesses under thermomechanical loading, $p_{\text{fs}} = 0$ (color online).

gradient index p_{fs} . Three models considered are 1-1-1, 1-2-1, and 2-1-2. The results indicate that the lower value of nondimensional transverse displacement \bar{w} is observed for the 1-2-1 sandwich structure, because the core is rich in ceramics ($p_{\text{core}} = 1$) and its thickness is twice as much as that of the face sheet. It is also seen that the nondimensional axial stress is in inverse relation to the face sheet gradient index, because the structure becomes rich in metal while the central deflection increases. The most rigid sandwich plate is 1-1-1 with a smaller value of central deflection. A higher value of nondimensional axial stress is obtained for the 1-2-1 FG sandwich plate.

Figure 2 plots the distribution of the dimensionless central transverse displacement along the x axis and the dimensionless axial, in-plane and shear stresses across the plate thickness. The plate has homoge-

neous upper and lower face sheets and an FGM core. Since the FGM core is symmetrical, the axial and in-plane stresses become zero at the center line, while the value of transverse shear stress $\bar{\tau}_{xz}$ is maximum at this point. It can be seen from the plotted curves that an increase in the core gradient index leads to an increase in the dimensionless axial $\bar{\sigma}_x$, transverse $\bar{\tau}_{xz}$ and in-plane $\bar{\tau}_{xy}$ shear stresses in the intermediate core layer. It is remarkable that the results are almost the same for the homogeneous face sheets independently of the p_{core} values. The dimensionless deflection is slightly influenced by the core material index because the face sheets are more rigid with a thickness twice as much as that of the core (1-1-1).

Figure 3 plots the transverse central displacement and stress variations versus the face sheet gradient index of the FG sandwich structure subjected to both

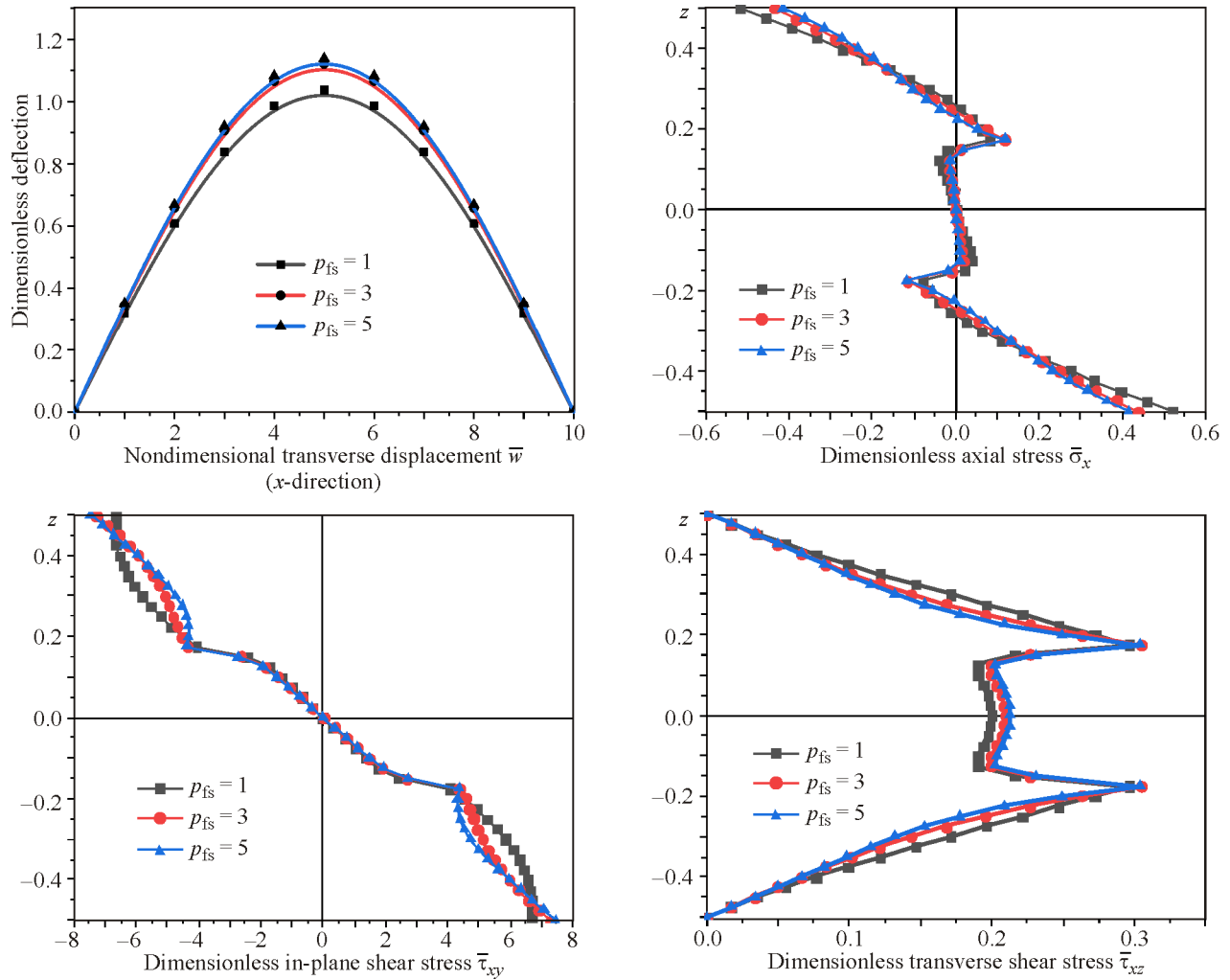


Fig. 3. Effect of the face sheet gradient index p_{fs} on the displacement \bar{w} and stresses $\bar{\sigma}_x$, $\bar{\tau}_{xy}$ and $\bar{\tau}_{xz}$ of the 1-1-1 sandwich structure subjected to thermomechanical loading, $p_{core} = 1$ (color online).

thermal and mechanical loading. The results indicate that the nondimensional central deflection increases with increasing face sheet gradient index p_{fs} , because the face sheets become rich in metal. The transverse $\bar{\tau}_{xz}$ and in-plane $\bar{\tau}_{xy}$ shear stresses increase with increasing face sheet gradient index at the surface and at the center line, respectively. Contrariwise, the axial stress is in inverse relation to the gradient index p_{fs} at the upper and lower faces of the FG structure. The present model gives a parabolic form of transverse shear stresses along the thickness direction. It can be concluded that the transverse $\bar{\tau}_{xz}$, axial $\bar{\sigma}_x$ and in-plane $\bar{\tau}_{xy}$ stresses are symmetrical about the center line because the scheme of the structure is symmetrical.

Figure 4 illustrates the effect of thermal load on the displacement \bar{w} and stress $\bar{\sigma}_x$, $\bar{\tau}_{xy}$ and $\bar{\tau}_{xz}$ distribution along the transverse direction of the FG sandwich structure under thermomechanical loading. It can be seen from the graphic results that all stress curves show a nonlinear distribution along the z axis (material gradient direction). An increase in temperature t_3 leads to an increase in the dimensionless values of axial $\bar{\sigma}_x$ and in-plane $\bar{\tau}_{xy}$ stresses. However, the distribution of the transverse shear stress $\bar{\tau}_{xz}$ is in direct relation to the nonlinear thermal parameter t_3 , indicating that the temperature rise has an impact on the flexural characteristics of the 1-1-1 FG sandwich plates. We can conclude again that the stresses are symmetrical because the material properties vary symmetrically about the center line.

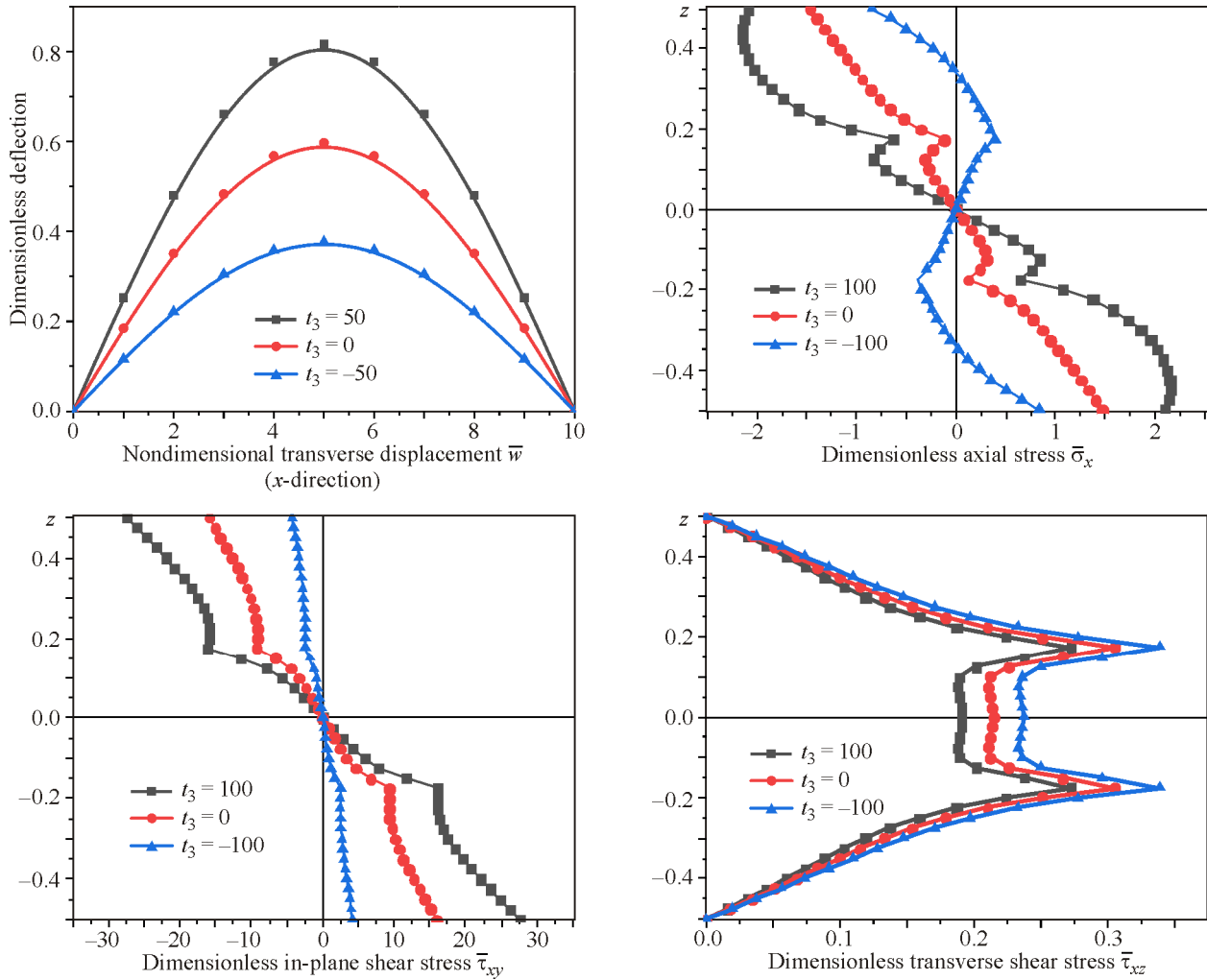


Fig. 4. Influence of the nonlinear thermal parameter t_3 on the displacement \bar{w} and stresses $\bar{\sigma}_x$, $\bar{\tau}_{xy}$, and $\bar{\tau}_{xz}$ of the 1-1-1 sandwich structure under thermomechanical loading, $q_0 = 100$, $t_2 = 100$ (color online).

6. CONCLUSIONS

The bending response of a uniform FG sandwich plate subjected to combined thermomechanical loading was investigated using a combined analytical exponential-cubic-sinusoidal integral HSDT theory. The flexural characteristics such as displacements and stresses were determined by solving governing differential equations derived from Hamilton’s principle. The validity of the proposed model was checked, and an excellent accuracy of the results and reduced computational time were achieved. The obtained results led to some important conclusions:

- The central deflection value is in direct relation to the face sheet gradient index because the index increases as the structure becomes rich in metal.

- The stresses along the thickness direction are nonlinear.

- The dimensionless axial and in-plane stresses are in inverse relation to the temperature parameter.

- An increase in the ceramic core thickness leads to a decrease in the deflection values because ceramics is more rigid.

Finally, it is necessary to account for the transverse shear effect, thermal load, material gradient variation and layer thickness in the sandwich structure calculation in order to correctly predict the structure dimensions in civil and mechanical engineering. To overcome the limitations of the current model, we can extend and improve the current formulation by including the thickness stretching effect in the calcu-

lation. The model can also be used for others materials, as shown in [51–59].

FUNDING

This work was supported by ongoing institutional funding. No additional grants to carry out or direct this particular research were obtained.

CONFLICT OF INTEREST

The authors of this work declare that they have no conflicts of interest.

REFERENCES

- Swaminathan, K., Naveenkumar, D.T., Zenkour, A.M., and Carrera, E., Stress, Vibration and Buckling Analyses of FGM Plates—A State-of-the-Art Review, *Compos. Struct.*, 2015, vol. 120, pp. 10–31. <https://doi.org/10.1016/j.compstruct.2014.09.070>
- Thai, H.T. and Kim, S.E., A Review of Theories for the Modeling and Analysis of Functionally Graded Plates and Shells, *Compos. Struct.*, 2015, vol. 128, pp. 70–86. <https://doi.org/10.1016/j.compstruct.2015.03.010>
- Dai, H.L., Rao, Y.N., and Dai, T., A Review of Recent Researches on FGM Cylindrical Structures under Coupled Physical Interactions, 2000–2015, *Compos. Struct.*, 2016, vol. 152, pp. 199–225. <https://doi.org/10.1016/j.compstruct.2016.05.042>
- Shen, H.S. and Li, S.R., Postbuckling of Sandwich Plates with FGM Face Sheets and Temperature-Dependent Properties, *Composites. B. Eng.*, 2008, vol. 39, no. 2, pp. 332–344. <https://doi.org/10.1016/j.compositesb.2007.01.004>
- Zenkour, A.M. and Sobhy, M., Thermal Buckling of Various Types of FGM Sandwich Plates, *Compos. Struct.*, 2010, vol. 93, no. 1, pp. 93–102. <https://doi.org/10.1016/j.compstruct.2010.06.012>
- Fazzolari, F.A., Natural Frequencies and Critical Temperatures of Functionally Graded Sandwich Plates Subjected to Uniform and Non-Uniform Temperature Distributions, *Compos. Struct.*, 2015, vol. 121, pp. 197–210. <https://doi.org/10.1016/j.compstruct.2014.10.039>
- Kashtalyan, M. and Menshykova, M., Three-Dimensional Elasticity Solution for Sandwich Panels with a Functionally Graded Core, *Compos. Struct.*, 2009, vol. 87, no. 1, pp. 36–43. <https://doi.org/10.1016/j.compstruct.2007.12.003>
- Alibeigloo, A. and Liew, K.M., Free Vibration Analysis of Sandwich Cylindrical Panel with Functionally Graded Core Using Three-Dimensional Theory of Elasticity, *Compos. Struct.*, 2014, vol. 113, pp. 23–30. <https://doi.org/10.1016/j.compstruct.2014.03.004>
- Liu, B., Ferreira, A.J.M., Xing, Y.F., and Neves, A.M.A., Analysis of Functionally Graded Sandwich and Laminated Shells Using a Layerwise Theory and a Differential Quadrature Finite Element Method, *Compos. Struct.*, 2016, vol. 136, pp. 546–553. <https://doi.org/10.1016/j.compstruct.2015.10.044>
- Natarajan, S. and Ganapathi, M., Bending and Vibration of Functionally Graded Material Sandwich Plates Using an Accurate Theory, *Finite Elem. Anal. Design*, 2012, vol. 57, pp. 32–42. <https://doi.org/10.1016/j.finel.2012.03.006>
- Neves, A.M.A., Ferreira, A.J.M., Carrera, E., Cinefra, M., Roque, C.M.C., Jorge, R.M.N., and Soares, C.M.M., Static, Free Vibration and Buckling Analysis of Isotropic and Sandwich Functionally Graded Plates Using a Quasi-3D Higher-Order Shear Deformation Theory and a Meshless Technique, *Composites. B. Eng.*, 2013, vol. 44, no. 1, pp. 657–674. <https://doi.org/10.1016/j.compositesb.2012.01.089>
- Thai, H.T., Nguyen, T.K., Vo, T.P., and Lee, J., Analysis of Functionally Graded Sandwich Plates Using a New First-Order Shear Deformation Theory, *Eur. J. Mech. A. Solids*, 2014, vol. 45, pp. 211–225. <https://doi.org/10.1016/j.euromechsol.2013.12.008>
- Nguyen, V.H., Nguyen, T.K., Thai, H.T., and Vo, T.P., A New Inverse Trigonometric Shear Deformation Theory for Isotropic and Functionally Graded Sandwich Plates, *Composites. B. Eng.*, 2014, vol. 66, pp. 233–246. <https://doi.org/10.1016/j.compositesb.2014.05.012>
- Akavci, S.S., Mechanical Behavior of Functionally Graded Sandwich Plates on Elastic Foundation, *Composites. B. Eng.*, 2016, vol. 96, pp. 136–152. <https://doi.org/10.1016/j.compositesb.2016.04.035>
- Zenkour, A.M. and Alghamdi, N.A., Bending Analysis of Functionally Graded Sandwich Plates under the Effect of Mechanical and Thermal Loads, *Mech. Adv. Mater. Struct.*, 2010, vol. 17, no. 6, pp. 419–432. <https://doi.org/10.1080/15376494.2010.483323>
- Wang, Z.X. and Shen, H.S., Nonlinear Analysis of Sandwich Plates with FGM Face Sheets Resting on Elastic Foundations, *Compos. Struct.*, 2011, vol. 93, no. 10, pp. 2521–2532. <https://doi.org/10.1016/j.compstruct.2011.04.014>
- Hirannaiah, S., Swaminathan, K., and Rajanna, T., Thermo-Mechanical Vibration and Buckling Analysis of Porous FG Sandwich Plates with Geometric Discontinuity Based on Physical Neutral Surface, *Mech. Adv. Mater. Struct.*, 2023. <https://doi.org/10.1080/15376494.2023.2220493>
- Kanu, N.J., Vates, U.K., Singh, G.K., and Chavan, S., Fracture Problems, Vibration, Buckling, and Bending Analyses of Functionally Graded Materials: A State-of-the-Art Review Including Smart FGMS, *Particul. Sci. Technol.*, 2019, vol. 37, no. 5, pp. 583–608. <https://doi.org/10.1080/02726351.2017.1410265>

19. Abbas, I.A. and Razavi, S.M.J., A Mode I Crack Problem for a Thermoelastic Fibre-Reinforced Anisotropic Material Using Finite Element Method, *Phys. Mesomech.*, 2018, vol. 21, no. 2, pp. 135–139. <https://doi.org/10.1134/S1029959918020066>
20. Petrova, V.E. and Schmauder, S., Modeling of Thermomechanical Fracture of Functionally Graded Materials with Respect to Multiple Crack Interaction, *Phys. Mesomech.*, 2017, vol. 20, no. 3, pp. 241–249. <https://doi.org/10.1134/S1029959917030018>.
21. Abouelregal, A.E., Sofiyev, A.H., Sedighi, H.M., and Fahmy, M.A., Generalized Heat Equation with the Caputo–Fabrizio Fractional Derivative for a Nonsimple Thermoelastic Cylinder with Temperature-Dependent Properties, *Phys. Mesomech.*, 2023, vol. 26, no. 2, pp. 224–240. <https://doi.org/10.1134/S1029959923020108>
22. Atta, D., Thermal Diffusion Responses in an Infinite Medium with a Spherical Cavity Using the Atangana–Baleanu Fractional Operator, *J. Appl. Comput. Mech.*, 2022, vol. 8, no. 4, pp. 1358–1369. <https://doi.org/10.22055/JACM.2022.40318.3556>
23. Jena, S.K., Chakraverty, S., Malikan, M., and Sedighi, H., Implementation of Hermite–Ritz Method and Navier’s Technique for Vibration of Functionally Graded Porous Nanobeam Embedded in Winkler–Pasternak Elastic Foundation Using Bi-Helmholtz Nonlocal Elasticity, *J. Mech. Mater. Struct.*, 2020, vol. 15, no. 3, pp. 405–434. <https://doi.org/10.2140/jomms.2020.15.405>
24. Sadovskii, V.M. and Sadovskaya, O.V., On the Acoustic Approximation of Thermomechanical Description of a Liquid Crystal, *Phys. Mesomech.*, 2013, vol. 16, no. 4, pp. 312–318. <https://doi.org/10.1134/S102995991304005X>
25. Palkanoglou, E.N., Baxevanakis, K.P., and Silberschmidt, V.V., Performance of Cast Iron under Thermal Loading: Effect of Graphite Morphology, *Phys. Mesomech.*, 2021, vol. 24, no. 5, pp. 598–610. <https://doi.org/10.1134/S1029959921050118>
26. Feldman, E. and Aboudi, J., Buckling Analysis of Functionally Graded Plates Subjected to Uniaxial Loading, *Compos. Struct.*, 1997, vol. 38, no. (1-4), pp. 29–36. [https://doi.org/10.1016/s0263-8223\(97\)00038-x](https://doi.org/10.1016/s0263-8223(97)00038-x)
27. Mahdavian, M., Buckling Analysis of Simply-Supported Functionally Graded Rectangular Plates under Non-Uniform In-Plane Compressive Loading, *J. Solid Mech.*, 2009, vol. 1, no. 3, pp. 213–225.
28. Chen, C.S., Chen, T.J., and Chien, R.D., Nonlinear Vibration of Initially Stressed Functionally Graded Plates, *Thin-Walled Struct.*, 2006, vol. 44, no. 8, pp. 844–851. <https://doi.org/10.1016/j.tws.2006.08.007>
29. Praveen, G.N. and Reddy, J.N., Nonlinear Transient Thermoelastic Analysis of Functionally Graded Ceramic-Metal Plates, *Int. J. Solids Struct.*, 1998, vol. 35, no. 33, pp. 4457–4476. [https://doi.org/10.1016/s0020-7683\(97\)00253-9](https://doi.org/10.1016/s0020-7683(97)00253-9)
30. Efraim, E. and Eisenberger, M., Exact Vibration Analysis of Variable Thickness Thick Annular Isotropic and FGM Plates, *J. Sound Vib.*, 2007, vol. 299, no. 4-5, pp. 720–738. <https://doi.org/10.1016/j.jsv.2006.06.068>
31. Zhao, X., Lee, Y.Y., and Liew, K.M., Free Vibration Analysis of Functionally Graded Plates Using the Element-Free kp-Ritz Method, *J. Sound Vib.*, 2009, vol. 319, no. 3-5, pp. 918–939. <https://doi.org/10.1016/j.jsv.2008.06.025>
32. Naderi, A. and Saidi, A., On Pre-Buckling Configuration of Functionally Graded Mindlin Rectangular Plates, *Mech. Res. Commun.*, 2010, vol. 37, no. 6, pp. 535–538. <https://doi.org/10.1016/j.mechrescom.2010.07.009>
33. Reddy, J.N., Analysis of Functionally Graded Plates, *Int. J. Numer. Meth. Eng.*, 2000, vol. 47, no. 1–3, pp. 663–684. [https://doi.org/10.1002/\(sici\)1097-0207\(200011/30\)47:1/3<663::aid-nme787>3.0.co;2-8](https://doi.org/10.1002/(sici)1097-0207(200011/30)47:1/3<663::aid-nme787>3.0.co;2-8)
34. Neves, A.M.A., Ferreira, A.J.M., Carrera, E., Cinefra, M., Roque, C.M.C., Jorge, R.M.N., and Soares, C.M.M., A Quasi-3D Hyperbolic Shear Deformation Theory for the Static and Free Vibration Analysis of Functionally Graded Plates, *Compos. Struct.*, 2012, vol. 94, no. 5, pp. 1814–1825. <https://doi.org/10.1016/j.compstruct.2011.12.005>
35. Reddy, J.N., A General Nonlinear Third-Order Theory of Functionally Graded Plates, *Int. J. Aerospace Light-Weight Struct.*, 2011, vol. 1, no. 1, pp. 1–21. <https://doi.org/10.3850/S201042861100002X>
36. Chen, C.S., Hsu, C.Y., and Tzou, G.J., Vibration and Stability of Functionally Graded Plates Based on a Higher-Order Deformation Theory, *J. Reinforc. Plastics Compos.*, 2009, vol. 28, no. 10, pp. 1215–1234. <https://doi.org/10.1177/0731684408088884>
37. Matsunaga, H., Free Vibration and Stability of Functionally Graded Plates According to a 2-D Higher-Order Deformation Theory, *Compos. Struct.*, 2008, vol. 82, no. 4, pp. 499–512. <https://doi.org/10.1016/j.compstruct.2007.01.030>
38. Thai, H.T. and Vo, T.P., A New Sinusoidal Shear Deformation Theory for Bending, Buckling, and Vibration of Functionally Graded Plates, *Appl. Math. Model.*, 2013, vol. 37, no. 5, pp. 3269–3281. <https://doi.org/10.1016/j.apm.2012.08.008>
39. Madenci, E., A Refined Functional and Mixed Formulation to Static Analyses of FGM Beams, *Struct. Eng. Mech.*, 2019, vol. 69, no. 4, pp. 427–437. <https://doi.org/10.12989/sem.2019.69.4.427>
40. Vinyas, M., On Frequency Response of Porous Functionally Graded Magneto-Electro-Elastic Circular and Annular Plates with Different Electro-Magnetic Conditions Using HSDT, *Compos. Struct.*, 2020, vol. 240, p. 112044. <https://doi.org/10.1016/j.compstruct.2020.112044>

41. Avcar, M., Free Vibration of Imperfect Sigmoid and Power Law Functionally Graded Beams, *Steel Compos. Struct.*, 2019, vol. 30, no. 6, pp. 603–615. <https://doi.org/10.12989/SCS.2019.30.6.603>
42. Gafour, Y., Hamidi, A., Benahmed, A., Zidour, M., and Bensattalah, T., Porosity-Dependent Free Vibration Analysis of FG Nanobeam Using Non-Local Shear Deformation and Energy Principle, *Adv. Nano Res.*, 2020, vol. 8, no. 1, pp. 37–47. <https://doi.org/10.12989/anr.2020.8.1.037>
43. Reddy, J.N., A Simple Higher-Order Theory for Laminated Composite Plates, *J. Appl. Mech.*, 1984, vol. 51, no. 4, pp. 745–752. <https://doi.org/10.1115/1.3167719>
44. Daouadji, T.H., Hadji, L., Analytical Solution of Non-linear Cylindrical Bending for Functionally Graded Plates, *Geomech. Eng.*, 2015, vol. 9, no. 5, pp. 631–644. <https://doi.org/10.12989/GAE.2015.9.5.631>
45. Kiani, Y., NURBS-Based Thermal Buckling Analysis of Graphene Platelet Reinforced Composite Laminated Skew Plates, *J. Thermal Stress.*, 2019, pp. 1–19. <https://doi.org/10.1080/01495739.2019.1673687>
46. Hadji, L., Influence of the Distribution Shape of Porosity on the Bending of FGM Beam Using a New Higher Order Shear Deformation Model, *Smart Struct. Syst.*, 2020, vol. 26, no. 2, pp. 253–262. <https://doi.org/10.12989/sss.2020.26.2.253>
47. Attia, M.A., On the Mechanics of Functionally Graded Nanobeams with the Account of Surface Elasticity, *Int. J. Eng. Sci.*, 2017, vol. 115, pp. 73–101. <https://doi.org/10.1016/j.ijengsci.2017.03.011>
48. Merzoug, M., Bourada, M., Sekkal, M., Ali Chaibdra, A., Belmokhtar, C., Benyoucef, S., and Benachour, A., 2D and Quasi 3D Computational Models for Thermoelastic Bending of FG Beams on Variable Elastic Foundation: Effect of the Micromechanical Models, *Geomech. Eng.*, 2020, vol. 22, no. 4, pp. 361–374. <https://doi.org/10.12989/gae.2020.22.4.361>
49. Rachedi, M.A., Benyoucef, S., Bouhadra, A., Bachir Bouiadjra, R., Sekkal, M., and Benachour, A., Impact of the Homogenization Models on the Thermoelastic Response of FG Plates on Variable Elastic Foundation, *Geomech. Eng.*, 2020, vol. 22, no. 1, pp. 65–80. <https://doi.org/https://doi.org/10.12989/gae.2020.22.1.065>
50. Bouhadra, A., Menasria, A., and Rachedi, M.A., Boundary Conditions Effect for Buckling Analysis of Porous Functionally Graded Nanobeam, *Adv. Nano Res.*, 2021, vol. 10, no. 4, pp. 313–325. <https://doi.org/10.12989/ANR.2021.10.4.313>
51. Yahea, H.T. and Majeed, W.I., Free Vibration of Laminated Composite Plates in Thermal Environment Using a Simple Four Variable Plate Theory, *Compos. Mater. Eng.*, 2021, vol. 3, no. 3, pp. 179–199. <https://doi.org/10.12989/cme.2021.3.3.179>
52. Cuong-Le, T., Nguyen, K.D., Hoang-Le, M., Sang-To, T., Phan-Vu, P., and Abdel Wahab, M., Nonlocal Strain Gradient IGA Numerical Solution for Static Bending, Free Vibration and Buckling of Sigmoid FG Sandwich Nanoplate, *Physica. B. Condens. Matter*, 2022, vol. 631, p. 413726. <https://doi.org/10.1016/j.physb.2022.413726>
53. Cuong-Le, T., Tran, L.V., Vu-Huu, T., and Abdel-Wahab, M., The Size-Dependent Thermal Bending and Buckling Analyses of Composite Laminate Microplate Based on New Modified Couple Stress Theory and Isogeometric Analysis, *Comp. Meth. Appl. Mech. Eng.*, 2019, vol. 350, pp. 337–361. <https://doi.org/10.1016/j.cma.2019.02.028>
54. Yaylaci, M. and Avcar, M., Finite Element Modeling of Contact between an Elastic Layer and Two Elastic Quarter Planes, *Comput. Concr.*, 2020, vol. 26, no. 2, pp. 107–114. <https://doi.org/10.12989/CAC.2020.26.2.107>
55. Ahmed, R.A., Fenjan, R.M., and Faleh, N.M., Analyzing Post-Buckling Behavior of Continuously Graded FG Nanobeams with Geometrical Imperfections, *Geomech. Eng.*, 2019, vol. 17, no. 2, pp. 175–180. <https://doi.org/10.12989/gae.2019.17.2.175>
56. Mehar, K. and Panda, S.K., Multiscale Modeling Approach for Thermal Buckling Analysis of Nanocomposite Curved Structure, *Adv. Nano Res.*, 2019, vol. 7, no. 3, pp. 181–190. <https://doi.org/10.12989/ANR.2019.7.3.181>
57. Timesli, A., Prediction of the Critical Buckling Load of SWCNT Reinforced Concrete Cylindrical Shell Embedded in an Elastic Foundation, *Comput. Concret.*, 2020, vol. 26, no. 1, pp. 53–62. <https://doi.org/10.12989/CAC.2020.26.1.053>
58. Selmi, A., Exact Solution for Nonlinear Vibration of Clamped-Clamped Functionally Graded Buckled Beam, *Smart Struct. Syst.*, 2020, vol. 26, no. 3, pp. 361–371. <https://doi.org/10.12989/SSS.2020.26.3.361>
59. Timesli, A., Buckling Behavior of SWCNTs and MWCNTs Resting on Elastic Foundations Using an Optimization Technique, *Phys. Mesomech.*, 2022, vol. 25, no. 2, pp. 129–141. <https://doi.org/10.1134/S1029959922020047>

Publisher’s Note. Pleiades Publishing remains neutral with regard to jurisdictional claims in published maps and institutional affiliations.